Harshavardhan Singh*, Sameen Azhar, Sanjukta Mandal, Sujit Kumar Mandal and Pamidiparthi Ravi Teja Naidu

An on-chip circular Sierpinski shaped fractal antenna with defected ground structure for Ku-band applications

https://doi.org/10.1515/freq-2021-0045
Received February 20, 2021; accepted May 20, 2021;
published online June 2, 2021

Abstract: In this paper, a circular Sierpinski shaped on-chip fractal antenna with defected ground structure (DGS) is presented for Ku-band applications. The fractal and defected ground structure are employed to achieve higher bandwidth for the entire Ku-band (12–18 GHz). The proposed on-chip antenna (OCA) with a footprint area of 4π mm^2 offers wide bandwidth of 7.22 GHz (11.94–19.13 GHz) with the resonating frequency of 15 GHz. At the resonating frequency, the designed antenna shows a peak gain of –19.76 dBi and a radiation efficiency of 55.6%. The co-polarization (CP) and cross-polarization ($\times P$) characteristics of the proposed OCA shows good isolation of 18.05 dBi and 17.44 dBi in the two principal planes with ϕ = 0° and 90° cuts respectively. The measured result of the designed OCA prototype shows a good performance over the desired frequency band.

Keywords: antenna miniaturization; defected ground structure; fractal antenna; gain enhancement; Ku-band; on-chip antenna.

1 Introduction

Integration of the large component like antenna and other RF front end circuits such as low noise amplifiers, voltage control oscillators, and power amplifiers on the same chip makes system on chip (SoC) technology-based devices truly compact and economical [1]. However, it becomes challenging to implement a standard $\lambda_0/2$ size antenna, especially for lower microwave bands like L, S, C, X, Ku, K with a frequency of less than 30 GHz. Because the operating wavelengths at these frequencies are much higher when compared to the small size chip area. Though a miniaturized antenna can be accommodated within the small chip area, it suffers from low gain due to significant aperture loss of the antenna. It is investigated that the lossy properties of silicon (Si) also cause substrate loss and reduce radiation efficiency [1]. Because of this low gain and efficiency, the SoC device with a smaller antenna is not used for long-distance communication [1, 2]. However, for short-range communication applications like intra and inter-chip communication [2], radio frequency identifications (RFIDs) [3], single-chip radar [4], defense systems [5], etc., these antennas offer flawless performances. By integrating two different on-chip antennas (OCAs) on Si wafer, a phased array is proposed for defense and satellite applications at a resonating frequency of 14 GHz with a bandwidth of 2 GHz in [5]. In [6], four on-chip antennas are integrated using 180 nm technology in a phased array system operating at 17 GHz with 2.4 GHz bandwidth. An on-chip synthetic aperture radar transceiver with a center frequency of 15 GHz and bandwidth of 1.45 GHz is reported in [7]. Various techniques based on fractal geometries such as bow-tie [8], Koch [9], and defected ground structure (DGS) [10] have been proposed to enhance the bandwidth of OCAs. The fractal bow-tie and Koch geometry-based OCAs are designed at 190 GHz and 60 GHz respectively, while the DGS based antenna is implemented at THz frequency. The reported higher bandwidth OCAs are designed to operate at higher frequencies, specifically with the resonating frequency greater than 60 GHz. However, to the best of the author's knowledge, the OCA with higher bandwidth and satisfactory radiation characteristics for lower microwave frequency remains to be addressed.

This work takes an opportunity to present an on-chip antenna covering the entire Ku-band with a frequency range from 12 to 18 GHz. To achieve the complete Ku-band from a CPW fed simple circular radiating patch; a

***Corresponding author: Harshavardhan Singh**, Department of Electronics & Communication, Microwave and Antenna Research Laboratory, National Institute of Technology Durgapur, Durgapur, India, E-mail: hsingh@ieee.org. https://orcid.org/0000-0001-9245-8630
Sameen Azhar, Sanjukta Mandal and Sujit Kumar Mandal, Department of Electronics & Communication, Microwave and Antenna Research Laboratory, National Institute of Technology Durgapur, Durgapur, India
Pamidiparthi Ravi Teja Naidu, Department of Space, Semiconductor Laboratory, Indian Space Research Organization (ISRO), Chandigarh, India

Sierpinski shaped fractal geometry is introduced in the patch radiator and two circular arc shaped DGSs symmetrical with respect to the feed line are implemented. The detailed design steps and consideration of the proposed OCA are discussed in Section 2. The analysis of the antenna performance and its characteristics with simulation and measured results have been presented in Section 3. Finally, a brief conclusion has been drawn in Section 4.

2 Design of on-chip antenna for Ku-band

2.1 Design consideration

The silicon (Si) based CMOS technology is the preferable choice to the semiconductor firms for fabricating ICs. The proposed OCA is designed using standard 0.18 μm CMOS technology. In the CMOS design layout, generally, 9–11 metal layers are sandwiched between the silicon dioxide (SiO_2) layers, as shown in Figure 1. The metal layers are made of aluminum, gold, or titanium. Copper is not recommended for on-chip applications to prevent contamination effects in a cleanroom environment. The SiO_2 layer is oxidized or deposited over the Si wafer depending upon the thickness of the layer. Generally, the antenna is designed on the top layer of the CMOS metal stack to achieve maximum radiation characteristics and reduce fabrication complexity. In this work, the proposed antenna is designed on the top metal layer. The top view and the layered view of the proposed antenna structure are depicted in Figure 2(a) and (b) respectively. The thin oxide layer between the bottom-most metal layer and low resistive Si wafer provides the isolation between them. The SiO_2 layer is also behaved as a mask to protect the Si surface from the impurity diffusion and acts as a passivation layer. Although the low resistive Si wafer is lossy, it is well suitable for designing other components of the ICs [1]. One can control the Si wafer resistivity by adding the doping substances, however, this would increase the additional design step and cost. The conventional planar antenna, like a microstrip patch embedded with low loss substrate, shows a very low bandwidth due to its high quality factor (Q-factor). The proposed OCA implemented on the lossy Si substrate is intended to operate over the complete Ku-band with a wide bandwidth of 6 GHz. To achieve such a wide band, a circular-shaped Sierpinski fractal is introduced on the circular radiating patch, and two circular arcs symmetric with respect to the CPW feed line are etched out from the ground.

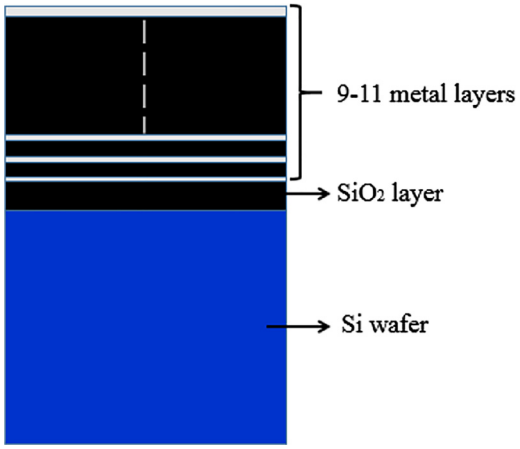

Figure 1: A standard layout of 0.18 μm CMOS technology.

2.2 Proposed design

The design steps of the proposed antenna with their respective electric field distributions are shown in Figure 3(a)–(e). Initially, a metal layer of thickness 'm_t' is stacked on the oxidized Si wafer with oxide thickness 'o_t'. Then, a simple circular patch of radius 'a' as shown in Figure 3(a) is designed with a resonating frequency of 15.27 GHz. To design both the ground and the radiating patch in the same plane, from the outer periphery of the circular patch, a circular slot of width 'g' is etched out which also isolate the patch and the remaining part of the outer periphery of the circular strip as shown in Figures 2(a) and 3(a). As the size of the OCA is too small to fit with the sub-miniature version A (SMA) connector for feeding with co-axial cable, a co-planar waveguide (CPW) feed excitation is chosen for exciting the antenna. The antenna with a CPW feed line of length 'f_l' and width 'f_w' is excited by a Ground Signal Ground (GSG) probe of 200 μm pitch. In the zeroth iteration, bandwidth of the patch antenna is obtained as 4.85 GHz covering from 12.85 to 17.7 GHz. Though this bandwidth is good enough for Ku-band application, with the aim of realizing higher bandwidth for the entire Ku-band, the Sierpinski fractal is introduced. The 1st to 3rd growth stages of the fractal structure are shown in Figure 3(b)–(d). Generation-wise, the radius of the circular slot of the fractal pattern is decreased as $a/4$, $a/8$ and $a/16$, where 'a' is the radius of the circular patch as shown in Figure 2(a). Finally, two circular arc shaped slots are etched out symmetrically with respect to the feed line. The arc angle 'θ' and width 'w' as indicated in Figure 2(a) are optimized for a resonance frequency of 15 GHz with a band width of 7.22 GHz. All the parameters of the proposed antenna are optimized for a resonating frequency of 15 GHz and their optimum values are listed in Table 1.

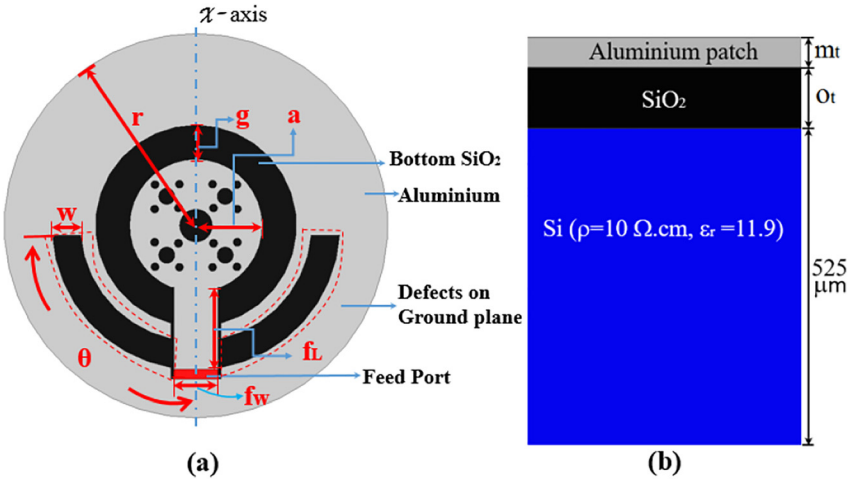

Figure 2: Proposed on-chip antenna. (a) Top view and (b) layered view.

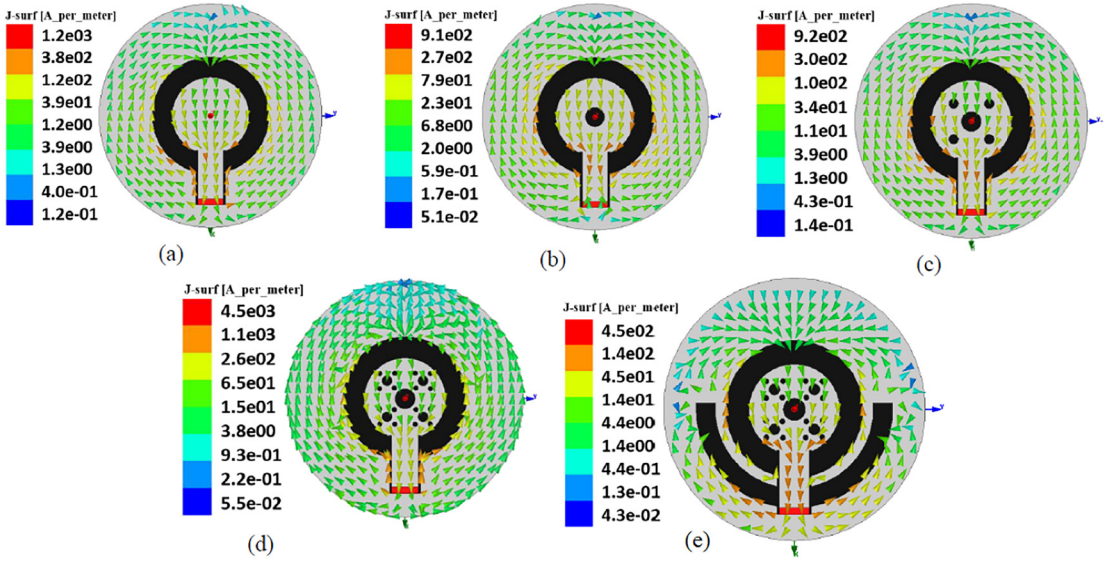

Figure 3: Stepwise improvement with vectored current distribution of the proposed antenna; (a) A CPW fed simple circular patch antenna, (b) the first generation stage, (c) the second generation stage, (d) the third generation stage of Sierpinski fractal, and (e) the antenna with two arc shaped DGS.

The stepwise S_{11} characteristics of the antenna are plotted in Figure 4. The resonance frequency, bandwidth and gain as obtained at each design steps are presented in Table 2. In the first iteration of the fractal structure, the bandwidth is increased by 450 MHz from 12.85 to 18.16 GHz. The bandwidth of the antenna is also increased in the second and third iteration of the fractal with 450 MHz and 310 MHz, respectively. From Table 2, it can be seen that due to the increase in electrical length of the patch at every growth stage of the fractal, the resonating frequency shifts towards left from 15.27 GHz in the 0th iteration to 15.13 GHz in the 1st iteration, then to 15.08 GHz in the 2nd iteration and, finally to 15.05 GHz in the 3rd iteration. The incorporation of the fractal pattern in the patch effectively reduces its aperture area which leads to reduce the antenna gain at each fractal growth stage. Further growth in the fractal stage leads to increase the design complexity. Therefore, the DGS with two arc shaped slots are created as the final design step of the proposed antenna. The DGS slot disturbs the current distribution in the ground plane, which affects the effective inductance and capacitance of the transmission line and leads to improve matching and enhance bandwidth [11]. The incorporated two arc slots in the ground help to achieve the entire Ku-band with a wide bandwidth of 7.22 GHz from 11.91 to 19.13 GHz. It is to be noted here that the inherent property of DGS in

Table 1: Optimized values of design parameters associated with the OCA.

Parameters	r	a	w	f_w	f_l	g	m_t	o_t	θ (°)
Values (mm)	2	0.69	0.3	0.45	0.83	0.36	1000	3000	87.37

conventional microstrip patch antenna enables back radiation which reduces the antenna gain [11]. However, here the radiation due to DGS is superimposed with the main lobe radiation and as an outcome, the gain of the proposed OCA is enhanced.

The vectored current distributions of the radiating and ground surfaces under each design step are shown in Figure 3(a)–(e). It can be observed that in all the design steps, the radiating patch is excited in its dominant TM_{110} mode. It can be seen from Figure 4 that at the resonant frequency of the respective design step, the impedance matching is progressively improved and with the incorporation of the DGS best matching is observed. As a result, the radiating patch excitation current density through the feedline is gradually increased after each design step and the maximum density of excitation current can be observed in the final step of the design. To see the designed antenna characteristics over the entire Ku band, the distribution of surface current density at different frequencies of the band is studied. For reference, the surface current density at the two cut-off frequency of the band (12 GHz and 18 GHz) and at resonant frequency (15 GHz) are depicted in Figure 5 (a, b and c). At all the frequency under consideration, the similar nature of the surface current density is noticed. This indicates that the designed antenna provides stable radiation characteristics throughout the band.

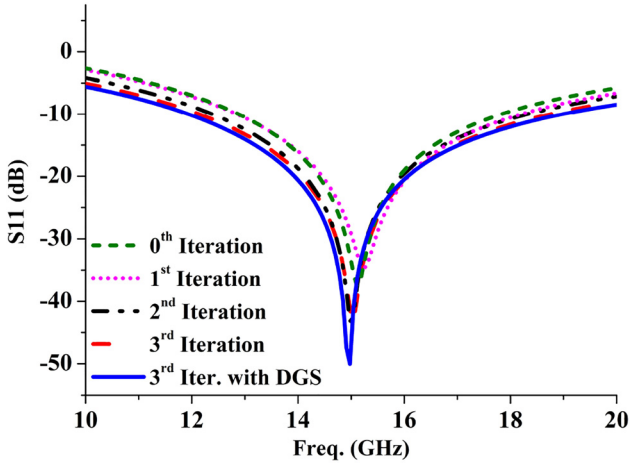

Figure 4: Return loss characteristics of the proposed OCA under each design step.

Table 2: Resonance frequency, bandwidth, and gain at each design step of the OCA.

Iteration	Resonance freq. (GHz)	Bandwidth (GHz)	Gain (dBi)
0th	15.27	4.85	−17.78
1st	15.13	5.3	−18.14
2nd	15.08	5.75	−18.36
3rd	15.05	6.06	−19.87
3rd with DGS	14.99	7.22	−19.76

2.3 Parametric analysis

The fabrication and integration of SoC devices on a single chip are sensitive towards its parameters. A small change in the simulated value of the parameter can lead to an undesired result. Thus, the analysis of certain parameters is generally asked by the IC manufacturing firm from the designers before going into fabrication process. Few important parameters are optimized parametrically and discussed below:

2.3.1 Feed width

The importance of feed line width in an antenna design is significant as it is logarithmically related to antenna impedance [12]. Figure 6 shows the variation in return loss when the feed width changes from 0.30 to 0.50 mm. It shows that best the matching of the feed line impedance with 50-Ω characteristic impedance is obtained at 0.45 mm and shows minimum reflection at this feed width. The impedance matching is significantly affected with the variation of the feed line width as with every change in the feed width of ±0.05 mm, the return loss is changed about 5 dB.

2.3.2 Oxide layer thickness (t_{ox})

Another parameter is oxide layer thickness which not only isolates the metal and Si wafer, it also provides an equivalent oxide capacitance (C_{ox}) and the capacitance between the metallic patch radiator and silicon wafer. This equivalent capacitance plays an important role in obtaining resonating frequency [2]. The oxide layer thickness also helps to reduce the antenna radiated field intensity towards the Si substrate and hence reduces substrate loss which enhances

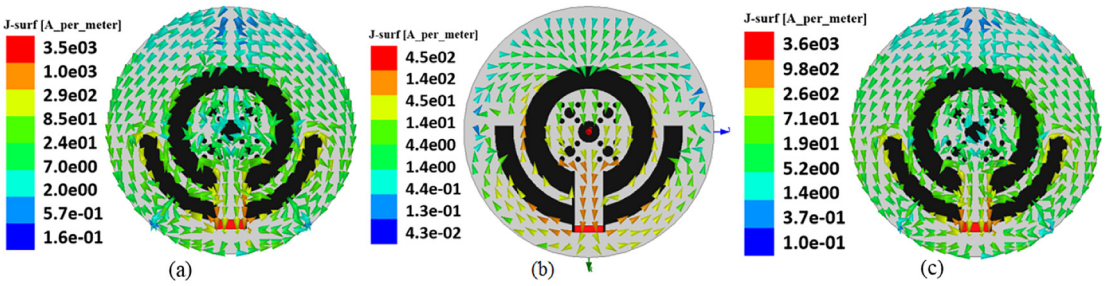

Figure 5: Analysis of current distribution of OCA for Ku-band. OCA at; (a) 12 GHz, (b) 15 GHz, (c) 18 GHz.

the antenna gain. For different values of SiO_2 thickness, the gain variation of the proposed OCA is plotted in Figure 7. It shows that the antenna gain varies from –22.98 to –19.76 dBi with higher thickness offering higher gain, when the oxide thickness, t_{ox} changes from 2 to 3 µm. Due to the limitation of the fabrication firm with 0.18 µm CMOS technology, the maximum thickness of 3 µm is taken. In the fabrication firm, where the prototype of the design is fabricated, the maximum oxide layer thickness of 3 µm can be achieved in one run time of the fabrication process using plasma enhanced chemical vapor deposition (PECVD) method. Though, with multiple run higher oxide layer deposition can be obtained, time consumption of the fabrication process restricts to one run. The oxide deposition rate of the PECVD tool used to fabricate the antenna is 25 min per micron.

3 Results and discussion

3.1 S_{11} characteristics

The S_{11} characterization set-up for the fabricated prototype of the proposed design along with the strip of the fabricated prototypes is shown in Figure 8. The setup consists of a CASCADE Summit 11000 AP probe station having metallic chuck, an electronic microscope, and a monitoring screen. Initially, the probe calibration is performed using short open load and thru (SOLT) test. Then, a 50 Ω RF micro-coaxial GSG probe is connected to the antenna under test (AUT). An electronic microscope and a monitoring screen are used to establish a proper connection between GSG and AUT. The simulated and measured S_{11} characteristics are plotted in Figure 9. The measured result of the fabricated prototype shows a large bandwidth of 8.19 GHz and it is higher as compared to the simulated bandwidth of 7.22 GHz. However, two deviations can be significantly observed from the measured characteristic curve.

Firstly, the operable frequency band is shifted towards the left side starting from 8.68 to 16.87 GHz instead of its desired Ku band of 12–18 GHz. Secondly, a glitch of –11.03 dB is appeared in the middle of the characteristic curve at 13.66 GHz.

One of the primary reasons for these deviations is the metal chuck of the probe station [1]. The prototype is placed on this metallic chuck and fed with a GSG probe of pitch size 200 µm. The metallic chuck not only acts as a spurious

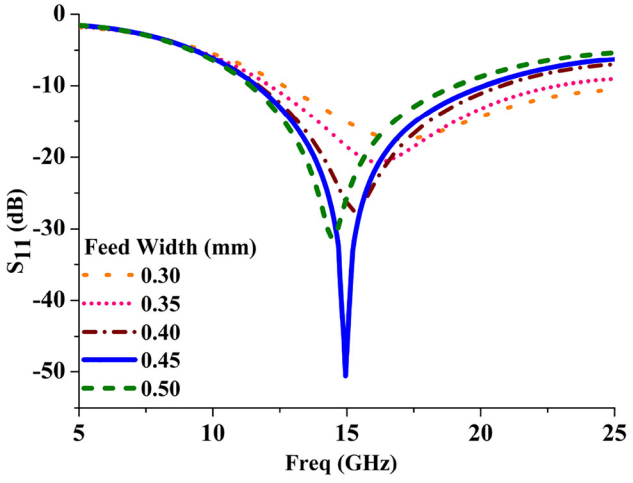

Figure 6: Change in return loss characteristics of the OCA with the variation of the feedline width at 15 GHz.

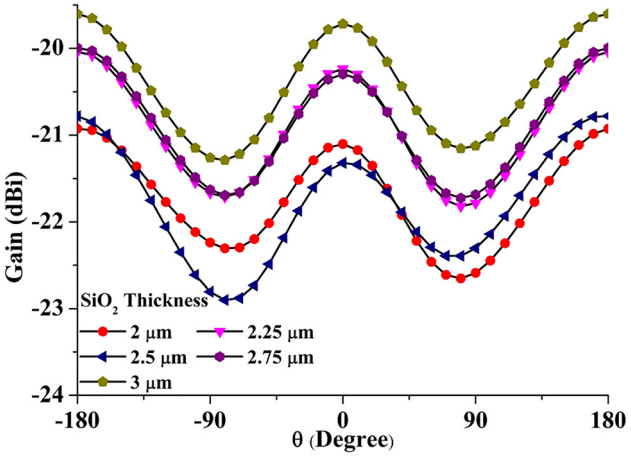

Figure 7: Variation of the OCA gain with the oxide layer thickness at resonating frequency 15 GHz.

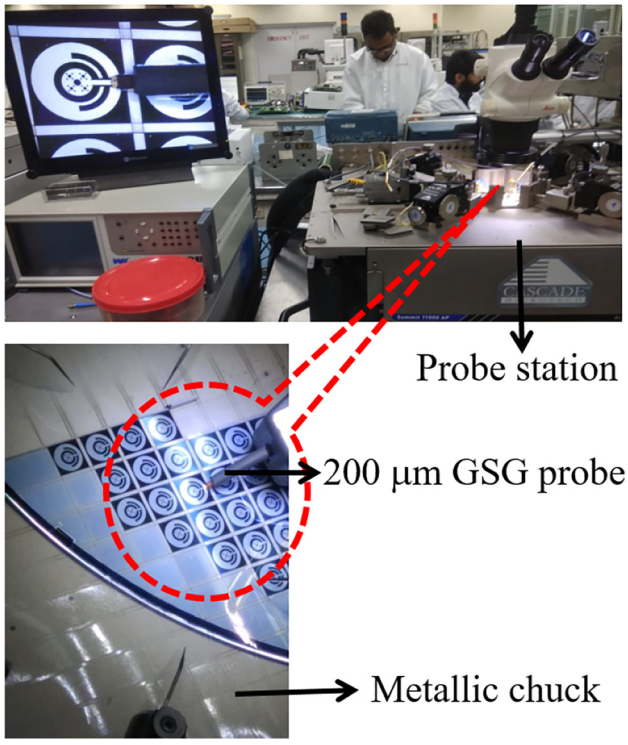

Figure 8: Return loss characterization set-up of the proposed OCA prototype (Courtesy: SCL).

ground for the CPW feed line of the antenna, but also leads to create a parallel plate wave guide structure which results in unexpected measurement results [13]. Also, the reflections and scattering effect from probes and nearby metallic objects produce the measurement errors [14, 15]. Moreover, the dissimilarity between material properties used for simulation and that for the fabrication can cause a difference in results [16]. However, a bandwidth of 8.19 GHz and 80% coverage of the desired band shows the closeness of the results to that of simulated one.

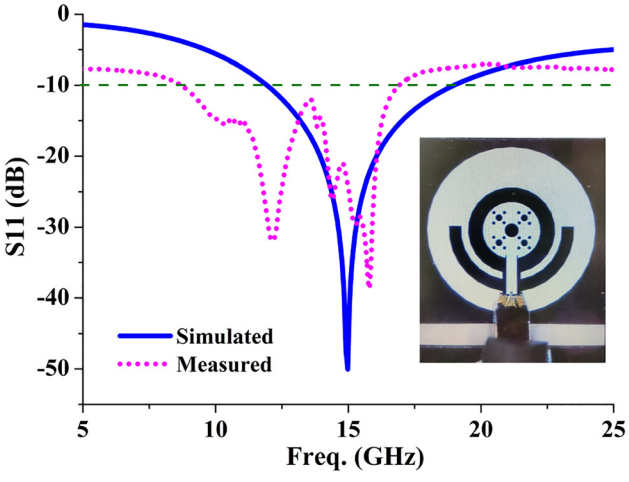

Figure 9: Simulated and measured return loss of proposed on-chip antenna along with the fabricated prototype micrograph with GSG feed (in inset).

3.2 Gain and efficiency

The simulated gain and efficiency of the proposed OCA are plotted in Figure 10. Over the complete Ku band, the antenna shows a good efficiency characteristic. The antenna efficiency lies between 38 and 55.6% which is relatively better as compared to the antenna reported in [17–19]. At the resonating frequency, the peak gain of the antenna is obtained as −19.76 dBi. However, on either side of the resonating frequency the gain is decreased. In the left side of the resonance frequency, the gain and efficiency are decreased due to the following three reasons. Firstly, with the decreasing frequency, the gain is decreased inversely square of the corresponding wavelength. Secondly, moving away from the resonance frequency towards both left and right side, the condition of impedance matching is deviated (Figure 4). Lastly, the loss associated with the Si substrate depends on frequency and with decreasing frequency it is increased the substrate loss is relatively less at higher frequency [20, 21]. Though with increasing frequency gain is increased and the substrate loss is decreased, however, significant impedance mismatch leads to decrease the overall antenna gain in the right side of the resonance frequency. Nevertheless, the proposed antenna gain, and efficiency are suitable for the short-range applications of the SoC based devices. An improvement in antenna gain can be realized with proper packaging of the antenna with other components of the complete system [22].

3.3 Co and cross polarization

In a low power SoC based device, the efficient use of the power helps to reduce the overall power consumption of the complete system. In an antenna, the power loss due to radiation in unwanted directions causes radiation loss and it degrades antenna gain and hence system performance in terms of power consumption. The co-polarization (CP) and cross polarization ($\times P$) characteristics of an antenna reflect the amount of power radiated in the desired and undesired desired planes. The CP and $\times P$ characteristics of the antenna in the two principal planes with $\phi = 0°$ and 90° cuts are presented in Figure 11. The CP and $\times P$ components in both of the planes are showing very good isolation of 18.05

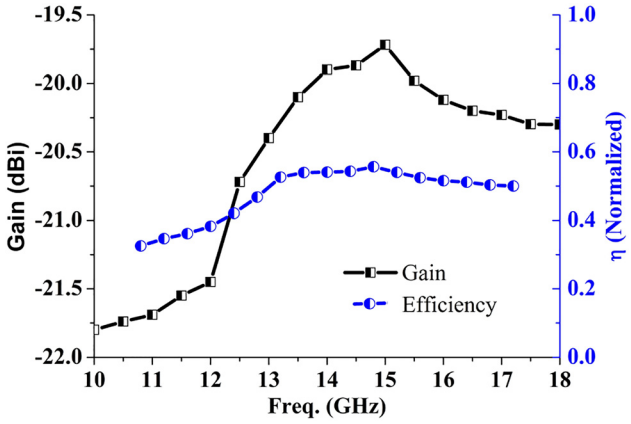

Figure 10: The simulated gain and efficiency characteristics of proposed OCA.

and 17.44 dBi respectively. This indicates a good polarization match and effectively less polarization loss. Hence, it makes the OCA more efficient for low power SoC devices used in Ku-band applications.

3.4 Comparative analysis

The comparative performance of the proposed antenna with some of the reported OCAs for lower range of microwave frequencies is mentioned in Table 3. The proposed antenna characteristics are compared in terms of substrate resistivity (ρ), size, gain (G) and efficiency (η). It can be seen that, for the same operating frequency (f_r) of the antennas reported in [23, 24], the use of high resistive substrate and SiGe HBT technology in [23] leads to realize higher gain as compared to the antenna with the low resistive substrate in [24]. Though high resistive substrate improves the antenna gain, it is already mentioned in previous Section 1, that the high resistive substrate materials are expensive and not commercially used for other circuits in the device. The on-chip antennas are mainly proposed for a short range wireless communication. The OCA gain ranging between −50 and −70 dBi is sufficient for clock and data distribution for intra- and inter-chip communication [19]. The proposed antenna with footprint area of 4π mm^2 shows a peak gain of −19.76 dBi and efficiency of 55.6% at resonating frequency. Along with that, a wide bandwidth of 7.22 GHz makes it suitable for high speed data communication.

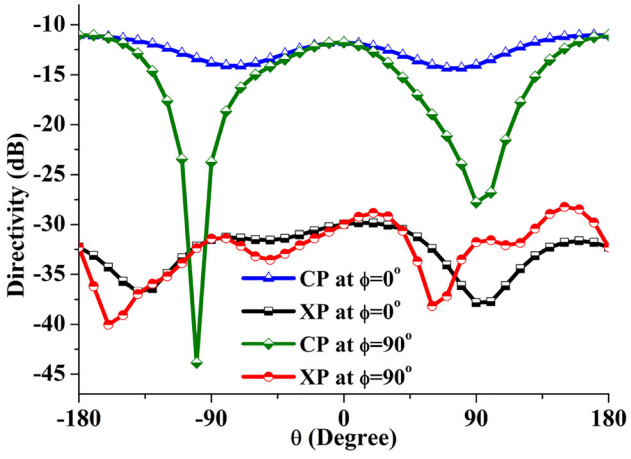

Figure 11: The simulated Co-pol and cross pol characteristics of OCA at 15 GHz.

4 Conclusion

The proposed Ku-band on-chip fractal antenna with defected ground structure exhibits significant characteristics to enable short range communication. A standard 0.18 µm CMOS process with a low resistive Si wafer is used for fabricating the prototype of the OCA. The Fractal and DGS techniques are successfully incorporated to achieve a wide bandwidth of 7.22 GHz for the entire Ku-band application. The measured result of the prototype shows a well compromised performance covering more than 80% of the desired frequency band. However, the performance of the measurement result can be improved by avoiding the metal based environment surrounding the antenna by using mm-wave absorbers and a wooden or insulated bottom chuck [25]. In the two principal planes with ϕ = 0° and 90° cuts, the simulation results of the OCA present a good isolation of 18.05 and 17.44 dBi between the CP and $\times P$ components. This assures the efficient design of proposed OCA.

Table 3: Comparison of proposed miniaturized OCA with the previously reported OCAs for microwave frequency range less than 24 GHz.

Ref.	OCA type	f_r (GHz)	ρ (Ω cm)	Size (mm^2)	G (dBi)	η (%)
[17]	Dipole	9	10^3	3.8 × 0.65	−26	36
[18]	Dipole	18	10^6	2 × 0.01	−36.5	NR
[19]	ZigZag dipole	15	20	2 × 0.02	−50	10.15
[23]	Folded dipole	24	10^3	2.1 × 0.9	−2	NR
[24]	Dipole	24	10	1.5 × 0.5	−8	NR
This work	Fractal patch	15	10	$\pi \times 2^2$	−19.76	55.6

Acknowledgement: The authors are thankful to Mr. Ayan Karmakar, Semiconductor Laboratory (SCL), ISRO, Chandigarh, India; for his help towards the fabrication and characterization of the proposed on-chip antenna prototype at SCL.

Author contributions: All the authors have accepted responsibility for the entire content of this submitted manuscript and approved submission.

Research funding: The authors gracefully acknowledge the financial support provided by Visvesvaraya PhD scheme, Ministry of Electronics and Information Technology (MeiTy), Govt. of India, Grant No. PhD-MLA/4(29)/2015-16/01.

Conflict of interest statement: The authors declare no conflicts of interest regarding this article.

References

[1] H. M. Cheema and A. Shamim, "The last barrier: on-chip antennas," *IEEE Microw. Mag.*, vol. 14, no. 1, pp. 79–91, 2013.

[2] H. Singh, S. Mandal, S. K. Mandal, and A. Karmakar, "Design of miniaturised meandered loop on-chip antenna with enhanced gain using shorted partially shield layer for communication at 9.45 GHz," *IET Microw, Antennas Propag.*, vol. 13, no. 7, pp. 1009–1016, 2019.

[3] S. Radiom, M. Baghaei-Nejad, K. Aghdam, G. A. E. Vandenbosch, L.-R. Zheng, and G. G. E. Gielen, "Far-field on-chip antennas monolithically integrated in a wireless-powered 5.8-GHz downlink/UWB uplink RFID tag in 0.18/SPL mu/m standard CMOS," *IEEE J. Solid State Circ.*, vol. 45, no. 9, pp. 1746–1758, 2010.

[4] B. A. Bedilu, P. T. M. van Zeijl, U. Johannsen, and A. Bart Smolders, "On-chip antenna integration for millimeter-wave single-chip FMCW radar, providing high efficiency and isolation," *IEEE Trans. Antenn. Propag.*, vol. 64, no. 8, pp. 3281–3291, 2016.

[5] D.-W. Kang, K.-J. Koh, and G. M. Rebeiz, "A Ku-band two-antenna four-simultaneous beams sige bicmos phased array receiver," *IEEE Trans. Microw. Theor. Tech.*, vol. 58, no. 4, pp. 771–780, 2010.

[6] X. Zhang, Y. Song, C. Yu, et al., "A ku-band phased array in package integrating four 180 nm cmos transceivers with on-chip antennas," in *2018 IEEE/MTT-S International Microwave Symposium-IMS*, IEEE, 2018, pp. 616–619.

[7] Y. Wang, L. Lou, B. Chen, et al., "A 260-mw Ku-band FMCW transceiver for synthetic aperture radar sensor with 1.48-GHz bandwidth in 65-nm CMOS technology," *IEEE Trans. Microw. Theor. Tech.* vol. 65, no. 11, pp. 4385–4399, 2017.

[8] B. Klein, P. Seiler, and D. Plettemeier, "On-chip fractal Bowtie-antenna for 185 GHz to 200 GHz," in *2015 IEEE International Symposium on Antennas and Propagation & USNC/URSI National Radio Science Meeting*, IEEE, 2015, pp. 1452–1453.

[9] S. M. A. Morais, A. J. R. Serres, I. S. Guarany, et al., "Aperture-coupled Koch fractal on-chip antennas for 60 GHz ISM band. in *2018 IEEE MTT-S Latin America Microwave Conference (LAMC 2018)*, IEEE, 2018, pp. 1–3.

[10] S. Gupta, B. K. Kanaujia, C. Dalela, and S. Patil, "Design of circularly polarized antenna using inclined fractal defected ground structure for s-band applications," *Electromagnetics* vol. 40, no. 7, pp. 526–540, 2020.

[11] D. Guha, S. Biswas, and Y. M. M. Antar, *Defected Ground Structure for Microstrip Antennas*. Microstrip and Printed Antennas, 2011.

[12] C. A. Balanis, *Antenna Theory: Analysis and Design*, 3rd ed. Hoboken, New Jersey., John Wiley & Sons, 2016.

[13] M. R. Karim, X. Yang, and M. F. Shafique, "On chip antenna measurement: a survey of challenges and recent trends," *IEEE Access*, vol. 6, pp. 20320–20333, 2018.

[14] L. Boehm, M. Hitzler, F. Roos, and C. Waldschmidt. Probe influence on integrated antenna measurements at frequencies above 100 GHz. in *2016 46th European Microwave Conference (EuMC)*, 2016, pp. 552–555.

[15] B. Klein, R. Hahnel, P. Seiler, M. Jenning, and D. Plettemeier. On-chip antenna pattern measurement setup for 140 GHz to 220 GHz. in *2015 IEEE International Conference on Ubiquitous Wireless Broadband (ICUWB)*, 2015, pp. 1–5.

[16] M. Nafe, A. Syed, and A. Shamim, "Gain-enhanced on-chip folded dipole antenna utilizing artificial magnetic conductor at 94 GHz," *IEEE Antenn. Wireless Propag. Lett.*, vol. 16, pp. 2844–2847, 2017.

[17] Y. Sun and A. Babakhani, "A wirelessly powered injection-locked oscillator with on-chip antennas in 180-nm SOI CMOS for spectroscopy application," *IEEE Sens. Lett.*, vol. 3, no. 7, pp. 1–4, 2019.

[18] A. B. M. H. Rashid, S. Watanabe, and T. Kikkawa, "High transmission gain integrated antenna on extremely high resistivity si for ulsi wireless interconnect," *IEEE Electron. Device Lett.*, vol. 23, no. 12, pp. 731–733, 2002.

[19] K. Kim, B. A. Floyd, J. L. Mehta, et al., "On-chip antennas in silicon ICS and their application," *IEEE Trans. Electron. Dev.*, vol. 52, no. 7, pp. 1312–1323, 2005.

[20] C.-Y. Hung and M.-H. Weng, "Investigation of the silicon substrate with different substrate resistivities for integrated filters with excellent performance," *IEEE Trans. Electron. Dev.*, vol. 59, no. 4, pp. 1164–1171, 2012.

[21] R.-Y. Yang, C.-Y. Hung, Y.-K. Su, M.-H. Weng, and H.-W. Wu, "Loss characteristics of silicon substrate with different resistivities," *Microw. Opt. Technol. Lett.*, vol. 48, no. 9, pp. 1773–1776, 2006.

[22] B.Dang, D.Liu, L.Marnat, A.Shamim, and C. K.-I.Tsang, "Package structures to improve on-chip antenna performance," US Patent 8,917,210, December 23, 2014.

[23] E. Ojefors, E. Sonmez, S. Chartier, et al., "Monolithic integration of a folded dipole antenna with a 24-GHz receiver in SIGE HBT technology," *IEEE Trans. Microw. Theor. Tech.*, vol. 55, no. 7, pp. 1467–1475, 2007.

[24] A. Shamim, L. Roy, N. Fong, and N. Garry Tarr, "24 GHz on-chip antennas and Balun on bulk si for air transmission," *IEEE Trans. Antenn. Propag.*, vol. 56, no. 2, pp. 303–311, 2008.

[25] D. Titz, F. Ferrero, and C. Luxey, "Development of a millimeter-wave measurement setup and dedicated techniques to characterize the matching and radiation performance of probe-fed antennas [measurements corner]," *IEEE Antenn. Propag. Mag.*, vol. 54, no. 4, pp. 188–203, 2012.